Journal of Nuclear Materials 389 (2009) 458–469

Contents lists available at ScienceDirect

Journal of Nuclear Materials

journal homepage: www.elsevier.com/locate/jnucmat

A US perspective on fast reactor fuel fabrication technology and experience part I: metal fuels and assembly design ☆

Douglas E. Burkes [a,*], Randall S. Fielding [a], Douglas L. Porter [a], Douglas C. Crawford [b], Mitchell K. Meyer [a]

[a] Idaho National Laboratory, Nuclear Fuels and Materials Division, P.O. Box 1625, Idaho Falls, ID 83415-6188, USA
[b] GE Nuclear – Global Nuclear Fuel, Wilmington, NC 28402-0780921, USA

ARTICLE INFO

Article history:
Received 2 September 2008
Accepted 24 February 2009

ABSTRACT

This paper is part I of a review focusing on the United States experience with metallic fast reactor fuel fabrication and assembly design for the Experimental Breeder Reactor-II (EBR-II) and the Fast Flux Test Facility (FFTF). Experience with metal fuel fabrication in the United States is extensive, including over 60 years of research conducted by the government, national laboratories, industry, and academia. This experience has culminated in a considerable amount of research that resulted in significant improvements to the technologies employed to fabricate metallic fast reactor fuel. This part of the review documents the current state of fuel fabrication technologies for metallic fuels, some of the challenges faced by previous researchers, and how these were overcome. Knowledge gained from reviewing previous investigations will aid both researchers and policy makers in forming future decisions relating to nuclear fuel fabrication technologies.

1. Introduction

There has recently been renewed interest in fast reactor fuels in the US and has resulted in the development of US Department of Energy Programs, such as the Generation IV Initiative [1,2], the Advanced Fuel Cycle Initiative [3], and the Global Nuclear Energy Partnership [4]. This interest has been spurred particularly by several global factors looming in the near future: consequences of the greenhouse effect that may prompt the implementation of a carbon tax, production of hydrogen and hydrogen-rich fuel cells to produce energy for transportation from hydrocarbons and water, increased demand for potable and irrigation water, proliferation concerns associated with separated Pu, and finding an alternative to a permanent spent fuel repository for minor actinides and long-lived fission products. Fast reactors are poised to effectively address these factors because fast reactor fuels provide adequate long-term management of Pu and the minor actinides, thereby minimizing proliferation risks and waste depository requirements, while still generating ample amounts of heat for energy, hydrogen, or water.

Safe and economical fuel fabrication is vital to the success of the aforementioned programs and continued interest in nuclear power generation in the US. Key considerations associated with selection and fabrication of fuels are reactor safety, satisfactory fuel performance at reactor operating conditions that meet goal outputs amenable to reprocessing, and overall system economics.

Technology for fabrication of fast reactor fuels has existed since the early 1960s and has continually been upgraded and refined over the past four decades. However, there is mounting concern that, with the rapidly diminishing levels of veteran researchers in the field and operational facilities associated with the research and development of metallic fuels, 40 years of experience will be lost and irretrievable to future researchers [5]. In addition, in order to keep nuclear power electricity as competitive as possible, improvements to the established fuel fabrication technologies should be continued along with innovative development of new fuels that are capable of performing under a wide range of operating conditions [6].

Fuel fabrication technologies should be specifically engineered with the desired properties incorporated into the nuclear fuel. There are certain material constraints, such as those created by fuel cladding and fuel element operating conditions and environment, which must also be considered prior to and during fabrication to maintain the cost effectiveness of nuclear fuels for fast reactors. The most desired properties of a fast reactor nuclear fuel are high fissile atom (^{235}U, ^{239}Pu) density, high thermal conductivity, and acceptable compatibility with the cladding and reactor coolant, minimized moderator concentrations, high melting point, and low swelling caused by fission products.

Constraints placed on cladding material selection are satisfactory creep and yield strength, adequate ductility following irradiation at refueling temperatures, low void swelling at high fast neutron doses, and acceptable compatibility with the fuel and

☆ This manuscript has not been published elsewhere and has not been submitted simultaneously for publication elsewhere.

* Corresponding author. Tel.: +1 (208) 533 7984; fax: +1 (208) 533 7863.
E-mail address: Douglas.Burkes@inl.gov (D.E. Burkes).

0022-3115/$ - see front matter © 2009 Elsevier B.V. All rights reserved.
doi:10.1016/j.jnucmat.2009.02.035

Table 1
Selected design parameters and results of EBR-I metal driver fuel loadings [13].

Core loading	First	Second	Third	Fourth
Fuel alloy (wt%)	HEU	U–2Zr	U–2Zr	Pu–1.25Al
Slug diameter (mm)	9.25	9.75	9.25	5.97
Cladding material	Ribbed SS347	SS347	Ribbed Zircaloy-2	Ribbed Zircaloy-2
Important result	Loss of reactivity with time	Partial melting of the core [14]	Improved stability of the fuel [15]	More compact core [16]

reactor coolant. The fuel cladding should perform well at high linear power, high heat ratings, and high surface heat fluxes with increased burnups[1] (10–20 at.%). In addition, the cladding should experience low distortion from swelling or bowing, have enhanced safety characteristics, and be fabricated in a way that does not inhibit reprocessing of the fuel.

This paper represents the first steps in documenting and reviewing established fast reactor fuel fabrication technologies and experience. This is part I of a two-part review of such technologies and experience, with emphasis placed on established technologies for metal fuels, because US experience with this fuel type is extensive. In addition, design and fabrication associated with reactor assemblies for both the Experimental Breeder Reactor-II (EBR-II) and the Fast Flux Test Facility (FFTF) are discussed. This review addresses key characteristics and components of the fabrication process, associated challenges, and how these challenges were overcome. For this reason, the review includes some detail concerning the processing/fabrication steps used previously and, in some cases, those still under development. The review represents the US's perspective on fuel fabrication technologies. Countries such as the United Kingdom [7], France [8], the Russian Federation, India, and Japan have continued to refine and expand on similar fuel fabrication technologies. From this standpoint, new questions arising from researchers and policy makers, both present and future, relating to the growth of nuclear technology through fuel fabrication and assembly are addressed.

2. Metal fuel fabrication technology

A brief review of the terminology used in this paper will be helpful, especially since efforts have been made to keep the terminology used here consistent with that of previous researchers, although the terms may be slightly different than those used today. The term 'slug' is defined as an un-encapsulated, as-fabricated piece of *metallic* fuel, also sometimes referred to as a fuel pin. The term 'fuel rod' is defined as the fuel capsule, also sometimes referred to as the fuel pin or fuel element. The term 'fuel column' is defined as a single fuel slug in this case, but more generally could be a stack of segmented fuel slugs.

2.1. History and experience

Early fast reactors in the US were fueled with metal fuel, including the Experimental Breeder Reactors, EBR-I (1951–1963) and EBR-II (1965–1994), in Idaho [9–11]. Metal fuels used in EBR-I consisted of unalloyed U and U–Zr and Pu–Al alloys, a summary of which is provided in Table 1. The LAMPRE-I (1961–1963) reactor was fueled with molten Pu–Fe alloy. The Enrico Fermi Reactor (Fermi I) in Michigan (1963–1972) was fueled with a U–Mo alloy [12].

2.1.1. EBR-II

A significant number (approximately 120,000) of metal fuel rods consisting of a U–5Fs alloy[2] (various designs designated as Mark-I, -IA and -II) were fabricated for use as driver fuel in EBR-II [12,17]. U–Zr binary alloys and U–Pu–Zr ternary alloys were also later used as driver fuel or proposed for driver fuel use and irradiated in EBR-II [11,18–20] and FFTF [21]. Alloying the metal fuel, which was often performed using Zr, was highly desirable because this raised the alloy solidus temperature, enhanced dimensional stability under irradiation, and reduced fuel cladding chemical interaction [22,23]. Metal fuel developments were mainly driven by economics relating to higher fuel burnups and ultimately led to the irradiation of approximately 90,000 Mark-I and -IA (U–5Fs) driver fuel rods [11]; more than 30,000 Mark-II (U–5Fs) driver fuel rods [18,24]; more than 13,000 Mark-III, -IIIA, and -IV (U–10Zr alloy), and more than 600 U–Pu–Zr alloy fuel rods [12] in EBR-II alone. The varied environments that the fuels were subjected to provided data that allowed fuel performance to be predicted in both steady-state and off-normal conditions [25,26] and related to design and fabrication parameters.

Approximately 35,000 of the fuel rods were remotely fabricated in the EBR-II Fuel Cycle Facility [11], and 24,000 metal fuel pins each were produced by Aerojet Nuclear and Atomics International during the Mark-I, -IA, and -II designs. A summary of the different metallic fuel designs used to fuel EBR-II is provided in Table 2. A summary of the fabrication campaigns associated with each of the designs in Table 2 is provided in Table 3.

The U–5Fs metal alloy provided sufficient phase stability, irradiation growth resistance, and allowable operating temperature range for irradiation in EBR-II, so long as the metal fuel did not exhibit a crystallographic texture that led to anisotropic growth during irradiation [27,28]. Crystallographic texture is commonly referred to as preferred orientation of grains (i.e. not random) that is induced by phase transformations of the alloy under stress or as a result of various mechanical treatments. Surface roughening is a related effect of crystallographic texture during repeated thermal cycling. Texture of the U–5Fs slugs was determined by X-ray diffraction at six locations in the sample fuel slug for the purpose of detecting the quenched-in gamma phase and by measuring and normalizing the reflected intensities from the (110) to the (021) [29]. A 1 h heat treatment was employed to convert gamma phase U to alpha phase, thereby minimizing any preferred crystallographic orientation that occurred in the U–5Fs metal alloy elements [30,31].

Texturing and quenched-in high-temperature phases were not issues with the latter fuels alloyed with Zr (U–10Zr and U–Pu–Zr). The high-temperature γ phase is not quenched as a metastable phase in these alloys; rather, 'martensite-like' α' and α'' phases form. The twinning that occurs to relieve stresses created by the transformation from the γ phase ensures very little quenched-in texture.

[1] Burnup is defined as the amount of heavy metal (i.e., U and higher actinides) in the fuel that has been fissioned. This measurement can be expressed as percent of heavy metal atoms that have fissioned (at.%) or in units of fission energy produced per metric ton of heavy metal (MTHM), e.g. GWd/MTHM or MWd/kgHM. One at.% of burnup corresponds to roughly 9.4 GWd/MTHM.

[2] Fissium (Fs) is nominally 2.4 wt% Mo, 1.9 wt% Ru, 0.3 wt% Rh, 0.2 wt% Pd, 0.1 wt% Zr, and 0.01 wt% Nb and designed to mimic the noble metal fission products remaining after a simple reprocessing technique based on melt refinement.

Table 2
Selected design parameters (nominal) of EBR-II metal driver fuel elements [18].

Design Fuel alloy (wt%)	Mark-I/-IA U–5Fs	Mark-II/-IIS/-IICS/-IIA/-IIC U–5Fs and U–10Zr	Mark-III/-IIIA U–10Zr	Mark-IV U–10Zr	Mark-V/-VA U–20Pu–10Zr
^{235}U enrichment (%)	52	67–78	66.9	69.6	Variable
Slug diameter (mm)	3.66	3.30	4.39	4.27	4.27–4.39
Fuel smeared density (%)[a]	85	75	75	75	75
Burnup limit (at.%)	2.6	8.9	10	N/A	TBD
Plenum-to-fuel volume ratio	0.18	0.68-1.01	1.45	1.45	1.45
Plenum gas	Inert	Inert	Inert	Inert	Ar
Cladding material	SS 304L	SS304L and SS 316	CW 316 and CW D9	HT9	HT9 and CW 316
Approximate number of total fuel rods fabricated	97,399	104,501	16,104	400	–[b]

[a] Smeared density is defined here as the ratio of the cross-sectional area of the as-fabricated fuel slug to the cross-sectional area defined by the cladding inner diameter.
[b] Conversion to the Mark-V/-VA fuel types was never started before EBR-II was terminally shut down in 1994.

Table 3
EBR-II fuel production, procurement, and manufacturing history.

Design	Dates	Approx. number of assemblies	Approx. number of fuel rods	Fabricator/location
First core	June 1960 – February 1961	176	10,781	ANL-E Coldline
Mark-IA	September1964 – April 1969	573	34,976	ANL-W Hotline
	October 1967 – December 1969	237	14,457	ANL-W Coldline[a]
	January 1967 – August 1971	366	22,358	Aerojet Nuclear
	July 1973 – February 1974	184	11,241	ANL-W Coldline[a]
	April 1975 – September 1975	58	3,586	
Mark-II	August 1969 – September 1969	12	780	ANL-W Coldline[a]
	November 1972 – June 1973	73	4,492	
	March 1974 – February 1975	277	16,945	
	May 1973–September 1976	396	24,200	Atomics International
	November 1975 – August 1976	110	6,749	ANL-W Coldline[a]
	April 1983–June 1986	153	9,367	
Mark-IIS	May 1981 – September 1981	9	549	ANL-W Coldline[a]
	March 1982 – July 1986	30	1,830	
Mark-IICS	October 1987 – May 1994	159	9,699	ANL-W Coldline[a]
Mark-IIA	March 1984 – December 1987	10	610	ANL-W Coldline[a]
	March 1985 – March 1986	30	1,830	
	April 1985 – July 1985	10	610	
	July 1985 – October 1985	6	366	Atomics International
	January 1986 – August 1987	5	305	ANL-W Coldline[a]
	March 1986 – June 1987	224	13,664	
	April 1986 – August 1988	20	1,220	
	August 1986 – May 1987	13	793	
Mark-IIC	July 1988 – May 1994	119	7,259	ANL-W Coldline[a]
	October 1989	46	2,806	
	June 1989 – January 1994	7	427	
Mark-III	July 1987 – October 1988	17	1,037	ANL-W Coldline[a]
	July 1987 – March 1989	34	2,074	
	December 1987 – November 1993	13	793	
	August 1988 – November 1989	6	366	
	March 1989 – April 1989	6	366	
Mark-IIIA	March 1989	1	61	
	June 1989 – November 1992	31	1,891	
	September 1989 – December 1993	34	2,074	
	November 1989 – December 1993	22	1,342	
	November 1992 – April 1994	100	6,100	
Mark-IV	October 1987 – November 1987	4	244	–[b]

[a] The ANL-W Coldline consisted of three main facilities: the Fuel and Assembly Storage Building, the Fuel Manufacturing Facility, and the Fuel Conditioning Facility, each used for varying processes and at different times for a given design.
[b] Only qualification assemblies were fabricated for the Mark-IV design; no standard driver fuel assemblies were made.

Impurity level amounts (200–500 ppm) of Si were alloyed with the Mark-I metal fuel to minimize the fission gas release, thereby minimizing the cladding stresses that occurred as the fuel swelled radially against the cladding and axially against engineered fuel lift-off restraints. Although minimized by techniques such as Si additions, these swelling-induced stresses led to limitations of the useful lifetime of Mark-IA metal fuels [9,12].

For the Mark-I and -IA fuel designs, the fuel element relied on an axial, column-type restrainer to secure the fuel slug position inside the cladding jacket, addressing a theorized 'lift-off' effect, or axial fuel motion occurring during irradiation. The restrainer rested on the top of the fuel column and extended through the fuel rod plenum contacting the upper end plug. The 'lift-off' effect was hypothesized to result from successive fuel swelling and cladding

contact as well as differential thermal expansion of the fuel, as the reactor started and shut down. The fuel-cladding contact and thermal gradients would cause the fuel slug to ratchet up the fuel column, further exacerbated by fuel creep during irradiation that would prevent the fuel from dropping to the original position during shutdown. The concern was that a sudden drop of the fuel slug in the cladding caused by specific reactor operating conditions would result in a sudden reactivity insertion, an obvious safety problem to reactor operation. However, the lift-off distance for any subassembly was 0.51–1.8 mm with the maximum lift-off distance between 0.5 and 6.4 mm at 2% burnup, posing no immediate safety problems for the reactor [32]. Furthermore, fuel lift-off was not observed for every fuel pin at various burnup levels; thus, the event appeared to be more random in nature as opposed to a common occurrence.

Aerojet Nuclear fabricated approximately 24,000 Mark-IA fuel elements (U–5Fs alloy) based on the general process described as follows. The vendor utilized centrifugal bonding as a sodium bonding technique rather than impact bonding. Centrifugal bonding takes advantage of a consistent, continuous centrifugal force to accomplish bonding of the sodium to the fuel slug, rather than utilizing sharp impacts generated by repeated contacts between the cladding tube and an anvil, such as that used for impact bonding that is described later. However, a deleterious texturing effect was found to occur upon irradiation of the centrifugally bonded U–5Fs fuel elements as a result of increased axial compressive stress typically not observed with impact bonding [30]. The fuel slugs were observed to shorten axially and expand radially, leading to an undesired loss in fuel reactivity in the reactor core and requiring compensation through control rod motion [33]. The texture effect was found to be rectified in a majority of the fuel elements (97.9% success rate) after heat treating the fuel elements at 660 °C [34].

Atomics International also fabricated approximately 24,000 Mark-II fuel elements beginning in mid-1973 [34]. The process was nearly identical to that employed on the ANL-W Coldline, but similar to Aerojet Nuclear, the contractor experienced problems with the injection casting, leak detection, and closure welding of the end plug to the jacket. The challenges associated with injection casting were attributed to the need for increased use of recycle material in alloy preparation and casting. The overall cumulative yield of the Atomics International injection casting process was only 62%. Issues with leak detection and closure welding were addressed by switching from a capacitance discharge (CD) process to a tungsten-inert-gas (TIG) process along with a programmable automatic welder with adequate success.

A series of restrainer designs were used during the course of the Mark-IA and various Mark-II-based fuel designs [35]. In the case of the Mark-IA fuel design, a column-type restrainer was used as discussed earlier. For the Mark-II based fuel designs three dimples were placed at equal distances around the cladding tube at the approximate mid-point of the fuel rod. Each dimple was approximately 1.65 mm in diameter located approximately 12.7 mm above the fuel column. Both restrainer designs, in some way, were observed to limit the useful lifetime of the fuel element. The restrainer designs were effective in preventing hypothesized lift-off, but were found to be unnecessary for Mark-III designs and subsequent designs because axial fuel motion was self-limiting [36]. The U–10Zr and U–Pu–Zr alloys also swelled due to fission gas bubbles, but the swelling was very predictable based upon Pu content (Pu additions resulted in lower axial swelling [37]) and no fuel slug lift-off was observed. Silicon additions were not made to these alloys. Silicon is considered an impurity in the Zr-alloyed fuel materials because it removes some of the Zr from solution by precipitating as a stable silicide. Soluble Zr increases fuel melting temperature, decreases fuel/cladding chemical interaction, and, therefore, is beneficial to fuel performance. Reduction of soluble Zr through precipitation of stable phases reduces these benefits. Oxygen, C, and N were similarly tracked as impurities in the U–Zr and U–Pu–Zr alloys because they also reduce soluble Zr by forming stable oxide, carbide, and nitride, or Zr precipitates stabilized by these impurities.

2.1.2. FFTF

Over 1,050 U–10Zr metal alloy fuel rods and 37 U–Pu–Zr fuel rods were irradiated in FFTF in addition to those irradiated in EBR-II [21]. Most of these were in a series of test assemblies (Metal Fuel in Fast Flux Test Facility or MFF series) designed to qualify HT9 clad U–10Zr metal fuel for FFTF standard driver fuel use. Ultimately, FFTF pursued $(U,Pu)O_{2-x}$ mixed oxide (MOX) fuel for driver assemblies rather than metal alloys.

2.2. Metal fuel fabrication process

Metal fuel has often been selected for use in fast reactors because it can be easily fabricated and has high thermal conductivity, high fissile and fertile density capability, and small Doppler reactivity feedback [38]. Furthermore, metallic fuels are easily recycled using melt refining or can be readily dissolved and electrorefined in a molten salt electrolyte. Electrorefining processes have been shown to remove fission products, allowing the return of the U, Pu, and minor actinides to the reactor, and, thus, may support an economical and proliferation-resistant reprocessing scheme [39,40].

2.2.1. Process overview

Metallic fuel slug fabrication process development progressed through a number of fabrication techniques and methods. The first core loading of EBR-I, termed Mk-I, was unalloyed, highly enriched U that was rolled and swaged to the desired final shape. The second (Mk-II) and third (Mk-III) core loadings of EBR-I were centrifugally cast U–Zr alloy and centrifugally cast U–Zr alloy coextruded with Zircaloy-2 cladding, respectively. The fourth and final loading of EBR-I (Mk-IV) was a centrifugally cast, NaK-bonded Pu–Al alloy [9]. The centrifugal casting process was similar to the centrifugal bonding process described earlier, except that the casting operation contained a vertical-tube vacuum induction furnace mounted directly over a vacuum-housed centrifuge. The molten alloy was poured into a central melt distributor and cast into molds rotating at the periphery of the apparatus. While the technique was encouraging, it was limited by the complicated and time consuming procedure, and required a significant number of manipulations to assemble and disassemble the furnace and molds.

The first loading of EBR-II driver fuel was U–5Fs fabricated by counter gravity injection casting and alloying unirradiated U with simulated fission products. The casting equipment had been designed for remote use in a hot cell [41]. The 'cold'[3] fuel casting was used to test the equipment design. The U–5Fs alloy represented the equilibrium alloy for the melt refining process to be used for reprocessing irradiated nuclear fuel [34]. The next fabrication campaign was done in a hot cell using reprocessed (melt refined) fuel as feedstock. Fuel was then fabricated in one of the ANL-W Coldline facilities (the Fuel and Assembly Storage Building, the Fuel Manufacturing Facility, or the Fuel Conditioning Facility) or by several commercial vendors.

Precision casting was the only method used for producing fuel slugs for use in EBR-II driver fuel, which ensured a non-textured structure and required a relatively short fabrication sequence with easy-to-build, easy-to-use equipment. It could be used in both a

[3] Within the paper, cold is defined as operations conducted outside of a remote cell, or as work conducted with non-irradiated materials, while hot is defined as operations conducted remotely, or as work conducted on irradiated materials.

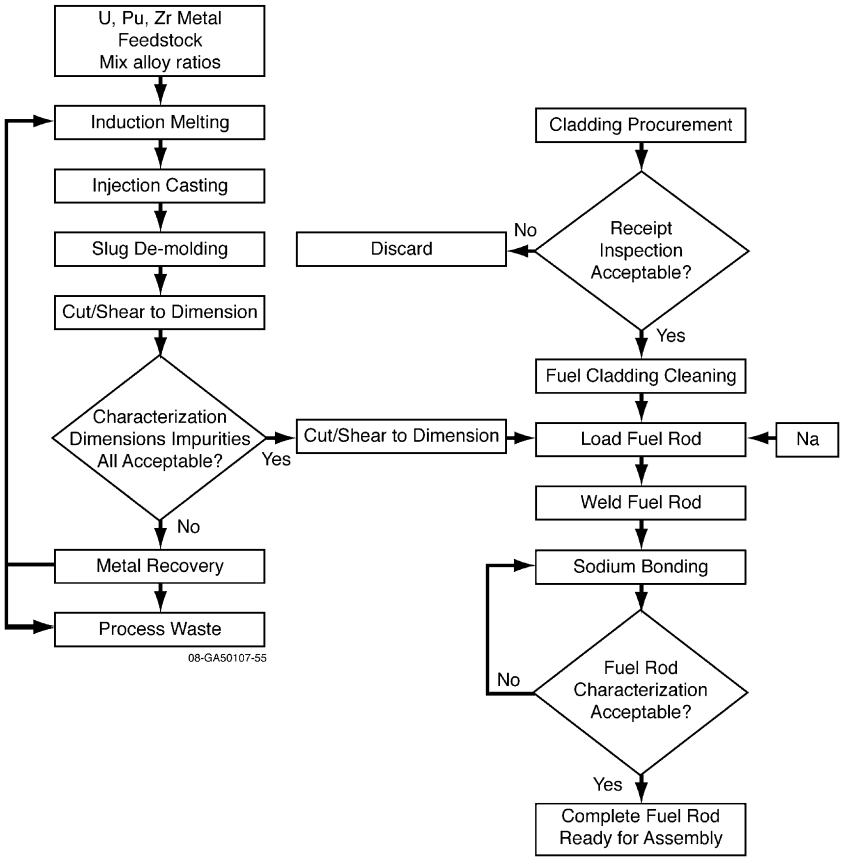

Fig. 1. Process flow diagram for fast reactor metal fuel fabrication.

cold prototype line as well as a hot reprocessing-production line. The fuel slugs designed and used during EBR-II and FFTF metal fuel irradiation testing were fabricated using precision casting. A typical process flow-sheet for fabricating precision cast fuel slugs is provided in Fig. 1. The following sections provide a more detailed review of the technology and experience relating to each of the steps shown in the figure.

2.2.2. Metal feedstock preparation from spent metallic fuel

Metal feedstock (U, Pu, and alloying elements) can be obtained from cold fuel inventories or taken from reprocessed fuel. In the latter case, this feed could be obtained by processing spent oxide or metallic fuels.

Two methods have been proposed and tested for metal feedstock preparation: (1) melt refining and (2) molten salt electrochemical reprocessing. Melt refining was an early reprocessing technique that melted spent fuel in a ZrO_2 crucible. The gaseous, alkali, alkaline earth, and rare earth fission products volatilized or oxidized to form a slag or 'dross', while the remaining U, Pu, and noble metal fission products were recovered and recast into fuel pins [13]. Molten salt electrochemical reprocessing is a currently used pyrometallurgical process that dissolves (in molten salt) and separates spent fuel from the undissolved cladding. The dissolved spent fuel is then electrolytically separated from the bulk of the fission products; the fuel products are deposited at the cathode, while most of the fission products remain in the salt [40,42]. Electrorefining produces a product that performs satisfactorily in a nuclear reactor, but it is also highly radioactive; thus, it is self-protecting and minimizes proliferation concerns [43]. An example of a Mark-IV anode and cathode containing reprocessed metallic constituents is provided in Fig. 2.

2.2.3. Injection casting

Initially, the U-Fissium was pre-alloyed, using conventional melt and pour techniques, to produce feedstock for injection casting. Later, the pre-alloying was eliminated and batches were composed of freshly enriched U, recycled chopped slugs, and/or heels from the injection casting process.

2.2.3.1. Pre-alloying. The high frequency induction furnace was designed to melt a 23 kg alloy batch under either vacuum or inert Ar gas up to a pressure of 345 kPa. The inert Ar gas atmosphere produced an ingot that was compositionally superior to that produced under vacuum. Each batch was brought up to 1,400 °C and held at this temperature for no more than 2 h for the U–5Fs alloys. This time period allowed for sufficient dissolution of the alloying elements into the U, resulting in a homogeneous mixture. After melting and homogenization, the material was tilt-poured into graphite molds. Two graphite mold designs were investigated for fuel ingot fabrication: a single cavity mold for a 10 kg ingot and a double cavity mold for two 10 kg ingots. The double cavity mold was preferred only because it reduced the number of castings and crucibles required. Zirconia-alcohol slurry was applied to the graphite molds before each pouring to coat the mold and, thus, reduce interaction between the melt and the graphite. A small portion of the melt (approximately 4%) that contained the undesirable fission products was allowed to oxidize in the crucible, forming the dross. The dross and any U recovered in an independent chemical process were removed after each alloy casting.

2.2.3.2. Combined casting process. As part of the Integral Fast Reactor fuels program in 1983, an improvement was made to combine the pre-alloying casting process (described previously) and the injection casting process (described hereafter) by mechanically stirring

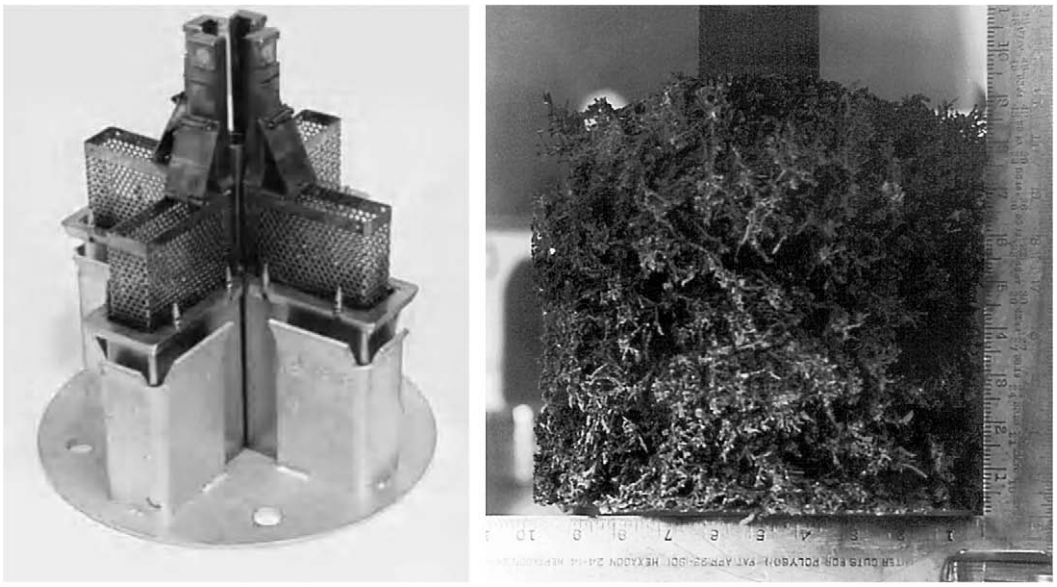

Fig. 2. Mark-IV electrorefiner anode (left) and cathode (right) containing the desired, reprocessed nuclear fuel constituents in metallic form.

the initial melt with a tantalum paddle to produce the chemically uniform molten alloy, then introducing the injection casting molds, pressurizing the furnace, and casting the final fuel slug product. The stirring improvement not only reduced the amount of time associated with mixing the feedstock components, but also aided in breaking up and dislodging thin layers of oxide that formed on the surface of the alloy melt during re-melt operations. Combining the alloying and injection casting steps into a single batch, with a single heat-up/cool-down cycle, simplified the process and reduced the impurities introduced into the final, as-cast fuel slugs.

The ingots of either pre-alloyed fuel feedstock (described previously) or feedstock elements to be alloyed, such as U and Zr or U, Pu, and Zr, were loaded into yttria-coated graphite crucibles and melted in a high-frequency-powered pressure/vacuum induction furnace at approximately 1,250 °C for U–5Fs alloys and approximately 1,500 °C for U–Pu–Zr alloys [44,45]. Placement of feedstock into the crucible was important to aid the alloying process. In an attempt to minimize material losses, Pu was loaded into the bottom of the graphite crucible, followed by Zr, and then U for U–Pu–Zr alloys. Zirconium was loaded into the bottom of the graphite crucible followed by U for U–Zr alloys. The idea was to allow the lower-temperature melting material (U) to flow over and consume the other (Zr). The outside of the graphite crucible was wrapped in zirconia felt to insulate the crucible from the induction coil and to prevent significant heat loss. The induction coil was made from a solid, oxygen-free, high-conductivity Cu bar, rather than Cu tubing, to effectively reduce resistive heating and serve as a heat sink because water cooling was not permitted inside the furnace shell. The mold pallet within the induction furnace was capable of holding up to 162 precision, bore-glass tubes used as molds, made of Vycor[4] or quartz. Although Vycor was used as the standard mold for Mark-I, IA, II, and IIS designs (U–5Fs), quartz was preferred for use with the 10 wt% Zr alloys (U–10Zr and U–Pu–Zr) due to the higher melt temperature of these alloys and the higher softening temperature of quartz (1,667 °C compared to 1,500 °C for Vycor) [46].

The molds were placed in a flanged opening directly above the melt crucible with vertical travel controlled by an air actuated cylinder. Each glass mold was internally coated with Zirconia-alcohol slurry and pre-heated prior to injection with a tubular heater in the furnace top hat. Yttrium oxide was also investigated as a coating for the glass molds, but was abandoned due to surface imperfections on the fuel slugs after casting. These imperfections were attributed to the water-based nature of the yttria slurry as opposed to the alcohol-based nature of the zirconia slurry.

The furnace was evacuated before each injection casting run. Following evacuation, the mold pallet was lowered, placing the lower portion of the molds below the surface of the melt. The molds were held below the melt surface for several seconds to allow the molds to pre-heat, after which the furnace was rapidly pressurized with Ar gas. The increased pressure rapidly forced the molten fuel alloy into the molds. The casting temperature and furnace pressure were controlled in such a manner that the molten alloy would fill the glass molds to within 25–51 mm. The furnace was allowed to cool below 300 °C before the castings were moved to a hood where the glass mold was broken, and the cast fuel slugs were removed.

Fuel slugs alloyed with Pu, and used for experiments, were cast and de-molded inside a glove box. The furnace inside the Pu glove box was capable of casting only 10–12 fuel slugs, and the mold pallet was manually raised and lowered. Each injection casting run typically required 4 h from initial loading to final unloading. The quartz molds had to be treated as contaminated waste because they were destroyed upon removing the cast metal fuel slugs, increasing the fabrication waste stream volume and cost. Of course, for the process to translate to a large-scale reprocessing/fuel fabrication facility, waste streams become a very important factor in process economics and public acceptance. An investigation into designing alternative molds that would remain intact as an integral part of the fuel slug was initiated to address this issue [47].

One initiative demonstrated the feasibility of reducing fabrication cost and waste stream requirements by using Zr mold material, which became an integral part of the cast metal fuel. In addition, Zr-sheathed fuel slugs exhibited significantly less axial elongation than did standard cast fuel slugs, while producing no significant increases in fission gas pressure or volume [48]. However, residual cracks were observed in the Zr metal periphery of the fuel slugs; thus, the mold does not serve as an adequate barrier to fuel/cladding interdiffusion.

2.2.3.3. Solidification defects. Although casting of metal fuel might appear to be a straightforward and well-refined process, challenges associated with quality and reproducible slug fabrication were

[4] Vycor is a trade name for the high-silica glasses from Corning Glass Works.

considered. A majority of these challenges were associated with solidification defects incurred during the injection casting phase. Such defects were manifested in the fuel castings as shrinkage pipes, microshrinkage, and hot tears as a result of improper casting temperature, geometry, directional and progressive solidification ratios, and extreme feeding distances [45].

Shrinkage pipes typically resulted from an imbalance between progressive shrinkage, created by radial solidification towards the center of the cast fuel rod, and directional shrinkage, created by axial solidification towards the heat source or melt pool. The result was pipe-shaped voids at various locations along the casting length. Careful balance between progressive and directional solidification fronts was required to eliminate these shrinkage pipes in the cast fuel. Control was performed in two ways: (1) maintaining a small axial temperature gradient from top to bottom through slow removal of the casting from the melt pool and (2) delaying the radial cooling that was created with an Ar gas purge along the mold walls until a strong directional solidification front was established. The molds remained in the molten pool until the submerged portion of the fuel slug was at a temperature below the alloy solidus.

Microshrinkage is characteristic of alloys with a wide freezing temperature range, such as those of interest in metal fuel applications. For example, a U–19Pu–10Zr alloy liquidus is at 1,300 °C while the solidus is at 1,080 °C, a 220 °C freezing range [49]. As explained for shrinkage pipes, solidification begins at the mold wall and upper, chilled end of the casting. Propagation of the solidification front occurred toward the thermal center of the casting. Grain growth simultaneously occurred in the partially liquid portion of the casting, creating an increasingly resistive path for molten metal to flow as grains continually grew. Microshrinkage occurred in areas of the casting where grain growth starved the shrinkage areas of molten metal. This defect became much more evident and challenging to overcome with increasing Pu contents in the fuel alloy, as the freezing range continued to widen. The void size created by microshrinkage was minimized by increasing the pressure over the molten pool during solidification. By increasing the pressure during casting and cooling, the feeding distance was effectively increased, which reduced the number and size of gas pores that were trapped at grain boundaries and, therefore, allowed an extended nucleation and growth process [50].

Feeding distance of a casting is a function of the casting diameter and the metal being cast. Therefore, feeding distance is critical for a liquid reservoir of metal to continually feed a solidification front. Metal fuel slugs typically had small diameters (Table 2) and high surface area-to-volume ratios, and the alloys had wide freezing ranges. Thus, increased feeding distance should increase microshrinkage effects, but this will be overcome by increasing the pressure inside the injection casting furnace.

Hot tears were another common fabrication challenge associated with injection casting. Hot tears occurred when an area of a casting was not allowed to shrink properly, placing the area under tension from metal contraction near the solidus temperature of the alloy [51]. The axially propagating solidification fronts contracted if cooling was initiated too quickly. Contraction of the metal between the fronts above the solidus temperature tore away from the solidified casting. Hot tears also resulted from diameter variations along the mold bore resulting in tension during solidification. Adjustments that reduced shrinkage pipe formation also reduced hot tears during solidification.

2.2.4. Fuel slug preparation and quality assurance

Fuel slugs were sheared to the appropriate length followed by quality control inspection for specified length, diameter, and mass. A commercial shear was used for the U–5Fs, U–10Zr, and low Pu content ($\leqslant$10 wt% Pu) U–Pu–Zr alloys, but was found to create uneven end surfaces when used to size high Pu content (>10 wt% Pu) U–Pu–Zr slugs due to the alloy's extreme brittleness. In this case, a simple tap of a small hammer on a chisel with a flat end surface was found to effectively shear the fuel slugs to length. It should be noted that conversion to U–Pu–Zr driver fuel elements was never started due to the shutdown of EBR-II. Length of the cast fuel slugs was measured by linear displacement of a linear variable differential transformer while the mass of each fuel slug was measured employing a commercial balance.

Fuel slug diameter was measured using an air gauge device from which back pressure was determined using a strain gage pressure transducer. Measured back pressure was proportional to the fuel slug diameter. The diameter was continuously recorded as the fuel slug was fed through the air gauge device so that an average diameter could be integrated over the nominal fuel slug length determined from the linear variable differential transformer, equating to a fuel slug volume. Experimentally cast fuels, or those cast on a smaller scale, such as the U–Pu–Zr alloys, were dimensioned using hand-held (glove-held) instruments.

Fuel slugs were examined using X-radiography to detect any internal defects such as voids and cracks. The composition and homogeneity of the fuel slugs were determined using chemical and isotopic analysis of samples taken from the top, center, and bottom of randomly selected fuel slugs.

2.2.5. Fuel rod fabrication

Fuel rods were fabricated after the fuel slugs had passed the inspections. A fuel jacket was fabricated, loaded with sodium to facilitate bonding, followed by the insertion of the fuel slug(s) and finally closure welded. The finished fuel rod was dimensionally characterized and He-leak checked. Welds were inspected both visually and radiographically for flaws. Details of the fuel element fabrication process are discussed as follows.

Fuel slug jackets are wire-wrapped cladding tubes with an end plug with either a stamped or machined tip welded into one end using an automated orbital gas tungsten arc welding (GTAW). Fuel slug jackets were fabricated from a variety of austenitic 304L, 316 (solution annealed 20% cold worked), and D9 (20% cold worked) stainless steels (SS) and the ferritic-martensitic HT9 SS (tempered Fe-12Cr-1Mo, similar to AISI 422). Chemical constituents of typical cladding materials are provided in Table 4. Rejection of cladding jackets was not uncommon during early rod fabrication designs as a result of inadequate inner-diameter discrepancies in the wire wrap and wire wrap weld to the tubing that resulted from operator error, material problems, or a combination of both, scratches, dents, pits, and/or spots on the jacket surface [34].

Mark-I and -IA cladding was fabricated from solution annealed 304L SS while solution annealed 316 SS was used for the Mark-II design, which was preferred because of improved swelling resistance and reduced interdiffusion at the fuel-cladding reaction layer [9,52,53]. The Mark-II fuel design incorporated other improvements upon the Mark-IA design, including a larger plenum capable of accommodating more fission gas and a reduced initial smeared density[5] to accommodate radial swelling of the fuel [53]. Both improvements effectively allowed increases in attainable fuel burnup without breach of the cladding.

As the capability to fabricate ternary metal fuels and the desire for higher burnups increased, jacket materials with enhanced resistance to fast neutron radiation-induced void swelling and creep were required, such as lower swelling D9 and HT9 alloys [54]. A summary of the peak diametral strain of the fuel rods as

[5] The fraction of the cross-sectional area internal to the cladding taken up by the fuel pellet cross section, determined from the following equation: 100% × (square of fuel outer diameter)/(square of cladding inner diameter).

Table 4
Elemental composition of typical alloys used for cladding in fast reactor fuel elements. Note that the irradiation database on Type PE-16 is limited [10].

Element	Nominal composition (wt%, balance Fe)			
	Type 316 austenitic	Type D9 austenitic	Type HT9 ferritic-martensitic	Type PE-16 Ni-based
C	0.08	0.05	0.20	0.10
Si	1.00	1.00	0.25	0.30
Mn	2.00	2.00	0.55	0.20
Ni	12.0	15.5	0.55	42.0
Cr	17.0	13.5	11.8	18.0
Mo	2.50	1.50	1.00	4.00
Ti	0.00	0.25	0.00	1.20
W	0.00	0.00	0.50	0.00
V	0.00	0.00	0.30	0.00
Al	0.00	0.00	0.00	1.20

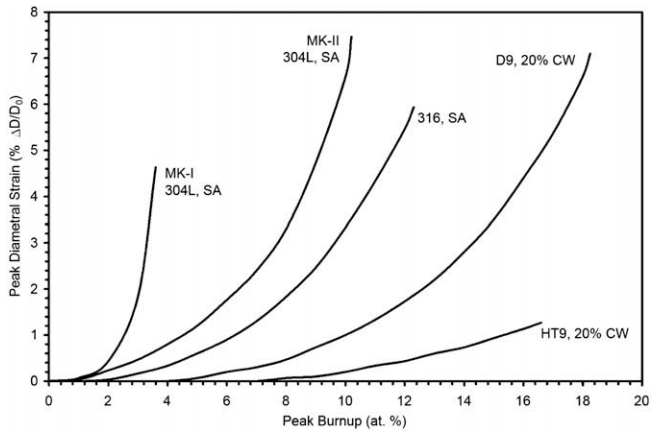

Fig. 3. Progressive improvement in the deformation swelling and creep measured by peak diametral strain as a function of peak burnup for the cladding materials of metallic fuel elements irradiated in EBR-II. SA, solution annealed; CW, cold worked [54].

a function of peak burnup for the different jacket materials is provided in Fig. 3.

HT9 cladding provided adequate resistance to both void swelling and to embrittlement at relatively high neutron doses, but the austenitic stainless steels, including D9, experience an extreme loss of alloy ductility at very high exposures upon swelling a significant amount ($\Delta V/V_o$ more than 10%) [55,56]. Although the HT9 cladding generally had the lowest diametral strain as a function of burnup compared to the other alloys in Table 4, the lifetime of HT9-clad fuel elements was limited at high operating temperatures (approximately 660 °C) due to inadequate high-temperature resistance to thermal creep induced by fission gas pressure [57,58].

Sodium loading, settling, and closure welding were carried out in a negative pressure Ar atmosphere (less than 50 ppm oxygen and water vapor) glove box; however, slight deterioration of the glove box atmosphere was desired for the duration of the sodium loading process to reduce the adhesiveness of the sodium. Sodium wires 3.2 mm in diameter were extruded and cut to the specified design length, based on the volume of sodium desired in the as-fabricated rod, using a shear. The wire was rolled by hand for straightening and to slightly reduce the diameter for ease in loading. The sodium wire was loaded into the fuel slug jacket through a funnel, and then the cast metallic fuel slugs were loaded. For EBR-II fuel elements, a single 34.3 cm long fuel slug was inserted into each jacket. Limitations to casting length required that two or three slugs be inserted to produce the 914 mm fuel column of FFTF fuel rods. Up to 50 fuel rods were loaded into a settling furnace, heated to 150 °C, and held at this temperature for several minutes to settle the fuel slugs into the molten sodium within the jackets. Settled fuel rods were removed to cooling racks for a minimum of 10 min. Heating the fuel elements from the bottom up was found to minimize ejection of the sodium caused by the expulsion of gas entrapped below the sodium surface. The upward flow of sodium from the bottom of the fuel to the annulus during the settling operation tended to be non-uniform and flowed in preferred channels, resulting in voids and pockets of entrapped Ar gas. The non-uniform flow was caused by non-uniform wetting of the sodium over the fuel or non-uniform pressure drops as a result of non-concentricity of the fuel element, producing an eccentric annular section [59].

Attempts were made to perform sodium settling under vacuum, but these attempts resulted in a rapid expansion of sodium in the small annular volume leading to deposition of sodium on the upper lip of the fuel rod. Vacuum settling also proved negative because gas occupying the preferred channels was readmitted after the vacuum was removed. Subsequently, the vacuum was determined to be unnecessary, and a simple low-temperature furnace was used for settling in two steps: to melt the sodium alone and then to heat it again after the fuel slug was introduced.

The fuel rods were closed by insertion and welding of the upper end plugs. The closure welding process originally employed a capacitance discharge technique [13,34] that fused the entire top of the end plug to the fuel rod jacket resulting in a hemispheric-shaped weld. Welding was carried out under flowing-Ar gas through the welding head. The capacitance discharge welding system consisted of a welding fixture with a frame to support an electrode holder, an element clamp, a gapping tool, an element positioning arm, and a power supply with approximately twenty 0.017 F capacitors. In 1973, Atomics International fabricated 13,000 Mark-II fuel elements employing a GTAW technique rather than the capacitance discharge technique. This change was successfully implemented to reduce the rejection rate encountered on a commercial fabrication scale. FFTF experimental fuel elements were also welded employing the orbital GTAW technique.

Leak testing of the welded fuel elements was performed using a pressure decay method. The leak-testing device consisted of a tight-fitting, O-ring-sealed chamber that was fit onto the weld, into which a metered amount of high-pressure He was injected [60,61]. The metered pressure, as measured by a pressure transducer, decreased if the welded fuel element had a leak allowing He from the chamber to be forced into the fuel rod. Settled and welded fuel rods were then removed from the glove box to an enclosed bonder for sodium bonding.

Sodium bonding is the process of wetting sodium to the fuel slug and cladding and removing any voids present in the annulus (the region between the fuel slug and cladding), each of which ensures adequate heat transfer between the fuel and cladding. Multiple bonding techniques were investigated, including furnace bonding, submerged canning, ultrasonic bonding, centrifuging, pressure pulsing, and vibratory bonding. Each of the techniques had significant advantages and disadvantages, and for the most part, each provided at least an 80% yield. However, only two techniques were capable of bonding a significant number of fuel rods simultaneously without the use of complicated equipment that could be susceptible to radiation damage-vibratory or impact bonding.

Two bonders were used, each containing four 2,000 W tubular heaters. Fuel rods were inserted into a bonder magazine that could accommodate up to 46 rods. The lower end of the fuel rod rested on an impact plunger. The bonder magazine was impacted 1,000 times at 500 °C. Fuel rod displacement was set to a specific range to provide the necessary amount of energy for sodium bonding without damaging the rod. Impacts needed to be sufficiently strong

to effect the movement of the fuel slug in order to remove voids present in the annulus [13]. The tubular heaters were allowed to cool below 90 °C from the bottom up, resulting in directional Na solidification, before removing the bonded fuel elements. Directional cooling was critical to reducing shrinkage voids in the excess sodium present above the fuel slugs [62]. Note that it was also important to begin the bonding cycle by heating from top to bottom to avoid melting sodium in the lower section because the still solid upper portion could not accommodate the thermal expansion.

An eddy-current bond tester was employed to determine the amount and quality of sodium bonding to the metallic fuel slugs. Specifically, the device was capable of detecting bubbles in the sodium, voids in the sodium-to-metal bond, sodium deposits clinging to the tube wall, and the location of the sodium meniscus above the fuel column [34]. The eddy-current bond tester monitored these specifications by inducing a current that flowed through the sodium annulus while measuring the change in resistance to the current flow. The eddy-current device was capable of detecting voids in the sodium of less than 1.59 mm in diameter. Voids less than 1.59 mm wide and 2.38 mm long were considered acceptable for insertion into the reactor; voids greater than this size would result in excessive fuel temperatures [63]. A typical readout from an eddy-current measurement is provided in Fig. 4. In addition, fuel rods were radiographed to determine closure-weld integrity and to confirm the sodium level.

Just before EBR-II was shut down in 1994, two decisions were made. The first was that eddy-current techniques were not perfect in catching bond defects out of specification, especially when HT9 cladding was used (HT9 is ferromagnetic at room temperature). Secondly, fuel slug and cladding dimensions were very consistent; the cladding was purchased to ±0.0013 cm tolerance on a 0.5080 cm inner diameter. If sorted into batches, the mold dimensions could also be kept uniform, with the sodium fill adjusted to the average dimensions of the batch. The consistency in dimensions, and ability to accurately weigh the bond sodium being added to the jacket, allowed the use of radiographically determined volumes of bond sodium in the fuel rod plenum to indicate whether a critical bond defect could exist in the fuel-cladding annulus. Knowing the fuel slug outer diameter and cladding inner diameter, a 2 cm debond along the fuel column will result in 0.5 cm of excess sodium in the gas plenum, assuming a 75% smeared density. This method is now suggested for production quality control if metal fuel fabrication is re-instated. Eddy current measurements are

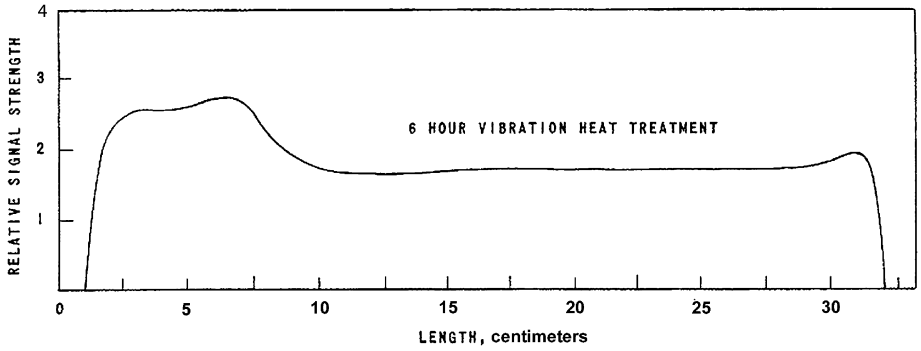

Fig. 4. Eddy-current trace of a well-bonded fuel rod. This particular fuel rod initially had defects after the bonding process, but the defects were alleviated after a 6 h vibration treatment at temperature [63].

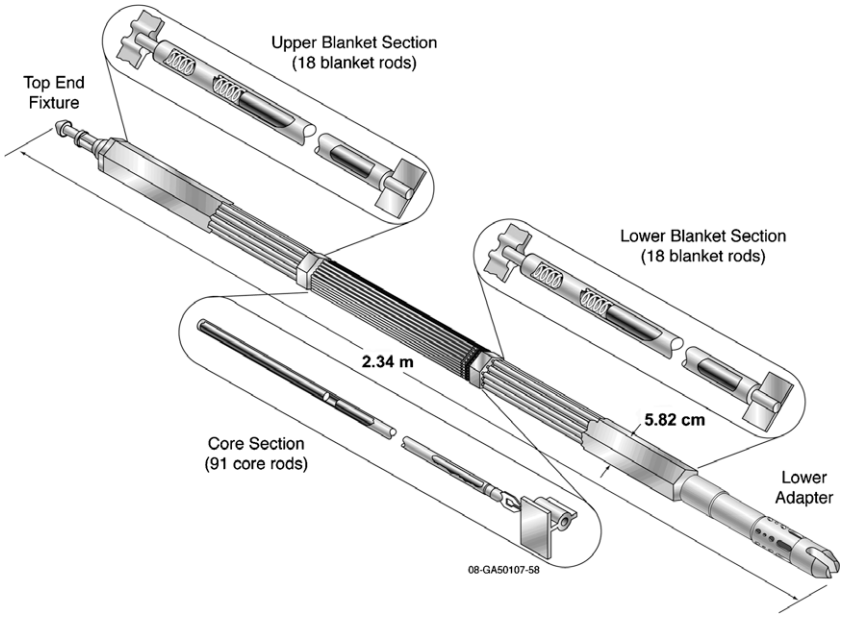

Fig. 5. EBR-II Core I driver fuel assembly schematic (early driver fuel assembly design).

therefore anticipated to be abandoned for future irradiation designs.

3. Assembly design and fabrication

The EBR-II Core I driver fuel assembly, a schematic of which is provided in Fig. 5, contained 91 fuel rods. Fuel rods were checked for straightness, damage to the tip, maximum dimensions through the welds, concentricity of the closure welds, dents, nicks, and abrasions prior to assembly fabrication. The fuel rods were arranged in a hexagonal array with the core section of each fuel assembly fitted with a top end fixture and a lower adaptor. The fuel rod tip was contoured in such a manner that allowed the tip to slide over a T-bar grid atop the lower assembly section.

For the EBR-II Core I fuel loading, assemblies were constructed remotely in a hot cell using a single pair of manipulators. Fuel assemblies were constructed in a vertical position because the temperature of the fuel rod, containing fuel processed using melt refining and, therefore, containing high concentrations of fission products, was above the melting temperature of sodium as a result of radioactive heating. An 2.4 m high structure supported fuel assembly equipment at three main levels. The upper level supported a set of guide rings and a cylindrical resistance heater; the middle level supported the fuel rod-loading equipment and equipment to clamp, heat, and cool the fuel rod bundle; and the lower level supported six pneumatically operated welding guns.

Fuel rods placed into the fuel assembly were held in a rack at the assembly station. The lower pre-assembly, containing axial blanket elements[6], was lowered into the station with a special grapple tool, positioned at the proper height, and clamped in place. A loading plate, containing a block with 11 loading guides, was positioned to align a set of matching T-bars with the T-bars on the grid plate (see Fig. 6) on top of the lower pre-assembly. A fuel rod was removed from the storage rack and placed in a loading cylinder and locked onto a guide wire. The fuel rod was then slid down the wire onto a T-bar on the loading plate. After a row of elements was assembled on the loading plate, the elements were slid onto the assembly grid. Fuel assembly rows of fuel elements were constructed in this fashion. Once all 91 fuel rods were in position, the fuel bundle was properly shaped using the clamps at the top and side of the assembly structure. The upper pre-assembly containing the hexagonal duct was lowered over the upper portion of the fuel bundle as the clamps were relaxed and lowered until the hexagonal duct tube was seated on the shoulder of the lower adaptor. The hexagonal tube was then welded to the lower adapter by six separate shielded-arc spot welding guns, with one weld on each face of the tube. Welds were specified as being able to withstand 13.3 kN, and every assembly was subjected to tensile load proof tests for quality assurance to ensure the assembly could withstand the 13.3 kN. Refer to reference [41] for an extended discussion of the fuel assembly fabrication process and associated equipment.

Fuel assemblies were tested for straightness with dial indicator readings taken at the axial center and top of each of the six hexagonal tube flats. A fuel assembly was considered 'straight' if there were no readings greater than 1.14 mm compared to a standard. Assemblies that failed this inspection were straightened with the manipulators and retested for compliance. All assemblies were flow tested to ensure there was no blockage and that the installation of the proper orificing would produce a given sodium coolant flow.

[6] Axial blankets were only used in the early versions of EBR-II assemblies, including those in the reprocessing era. Stainless steel reflector blocks replaced the blanket fuel in all other designs.

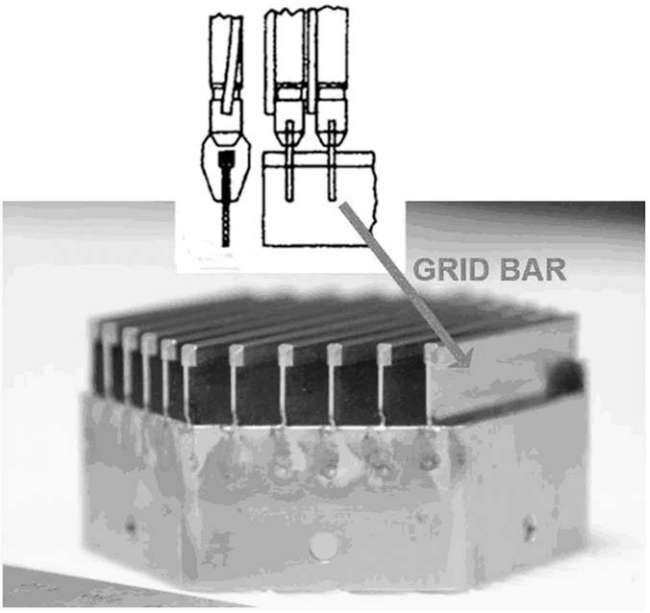

Fig. 6. Grid bar assembly used in an EBR-II driver fuel assembly to assemble a 91-pin assembly of Mk-II fuel rods. The insert shows how the fuel pins were arranged on a grid bar using a 'spade' on the lower end plug.

Table 5
EBR-II and FFTF driver fuel assembly design features for use with metal (EBR-II) and MOX[b] (FFTF) fuel [64].

Dimension	EBR-II	FFTF
Overall length, cm	232.8	365.8
Flat-to-flat OD (hex duct diameter), cm	5.809 5.888-at load pad	11.621 11.976-at load pad
Duct wall thickness, cm	0.102	0.305
Duct material	304SS, 316SS	316SS
Number of fuel pins	91, 61	217
Fuel	U–5Fs, U–10Zr	MOX: two-zone compositions[a]
Fuel column, cm	34.3	91.44

[a] Note that the series-III.b FFTF driver fuel (planned) was to be U-10Zr metallic fuel, the duct made from HT9 [65].
[b] The second part of this paper deals with ceramic fuel fabrication technology, including MOX, and can be found in reference [67].

Note that while these were the typical assembly techniques in the hot cell, assembly was similar, but all hands-on, for all other EBR-II driver fuel designs. The bundle of elements was first assembled horizontally. The quality inspections were also similar, but dimensional inspections were obviously much easier to perform and straightness could be accurately measured along the length of the assembly. Typical EBR-II and FFTF driver fuel assembly dimensions are shown in Table 5.

FFTF assemblies were of similar design incorporating a hexagonally-shaped fuel bundle and hex duct and flow was controlled using an orifice block in the lower reflector (see Fig. 7). Despite the dimensional differences the fabrication steps were very similar. The bundle was assembled in a horizontal position, and the assembly was assembled in a vertical position. The final weld for the hex duct was made directly to the lower reflector pre-assembly.

When designs had been developed to the point where using HT9 stainless steel for hex ducts was feasible, the welding of duct to pre-assembly became problematic, either because of welding dissimilar stainless steels (EBR-II pre-assemblies were constructed from 304 SS) or the brittle nature of as-welded HT9-to-HT9 weld-

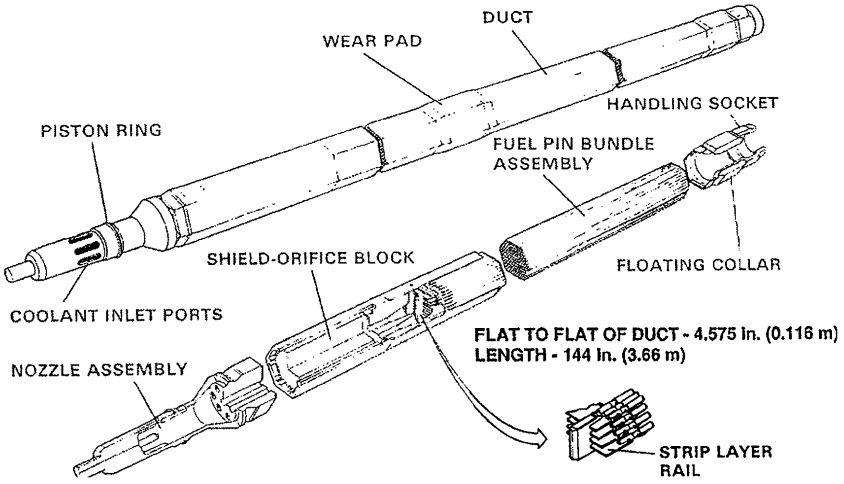

Fig. 7. Schematic of a series I FFTF driver fuel assembly [65].

ment. Mechanical attachments were designed to resolve these issues, which also resulted in significant economical savings. One of the greatest challenges yet to be overcome with increasing fast reactor fuel system lifetimes is minimization of distortion in the fuel bundle duct materials. Distortions lead to pin bundle-to-duct interference and increased withdrawal loads from the core as a result of duct swelling and bowing [66]. Note that all EBR-II driver fuel designs subsequent to the Mark-IA were eventually life-limited by duct dilation, caused by swelling and creep of the duct material, and not by the breach characteristics of the fuel. FFTF resolved the issue of duct dilation by adding a wear plate to the fuel assembly, minimizing the section of duct that was in contact with adjacent ducts so that slightly more distortion could be allowed.

4. Summary

The US's experience with metallic fast reactor fuel fabrication technology is extensive. This experience has been gained through the diligent efforts of numerous organizations, such as the government, national laboratories, industry, and academia. It is important to note that the fabrication techniques were easily adapted to and demonstrated for remote, hot cell use as early as 1964, and improvements continued through the early 1990s. It is imperative that the experiences gained from 1947 through today, with a slow down in the 1990s, be well documented and understood so that future researchers can easily access and understand this information. As the energy crisis and proliferation risks throughout the world continue to grow, nuclear energy must maintain its status as a solution to the problem and become even more competitive. A critical path toward the nuclear energy renaissance is and will continue to be fuel fabrication. Technologies that improve the quality, enhance the safety, and reduce the cost associated with nuclear fuel fabrication should continually be sought and should build upon the established technologies and traditions of previous researchers documented in this paper.

US Department of energy disclaimer

This information was prepared as an account of work sponsored by an agency of the US Government. Neither the US Government nor any agency thereof, nor any of their employees, makes any warranty, express or implied, or assumes any legal liability or responsibility for the accuracy, completeness, or usefulness of any information, apparatus, product, or process disclosed, or represents that its use would not infringe privately owned rights. References herein to any specific commercial product, process, or service by trade name, trademark, manufacturer, or otherwise, does not necessarily constitute or imply its endorsement, recommendation, or favoring by the US Government or any agency thereof. The views and opinions of authors expressed herein do not necessarily state or reflect those of the US Government or any agency thereof.

Acknowledgements

The authors wish to acknowledge the many scientists, engineers, technicians, and support staff involved with the EBR-II and FFTF over three decades. Their commitment, integrity, and knowledge has in no small part inspired a new generation of scientists, engineers, technicians, and support staff to continue the great and important work they established, especially in such a dire time of need. This work is supported by the US Department of Energy, Office of Nuclear Energy (NE), under DOE Idaho Operations Office Contract DE-AC07-05ID14517.

References

[1] A Technology Roadmap for Generation IV Nuclear Energy Systems, Issued by the US DOE Nuclear Energy Research Advisory Committee and the Generation IV International Forum, 2002, (Available through the US Department of Energy).
[2] US Department of Energy Office of Nuclear Energy, Science and Technology, The US Generation IV Implementation Strategy, 2003.
[3] US Department of Energy, Report to Congress on the Advanced Fuel Cycle Initiative, 2003.
[4] US Department of Energy, Press Release, Department of Energy Announces New Nuclear Initiative, 2006.
[5] The 33rd IAEA International Working Group Meeting on Fast Reactor, Recommendations, IWG-FR, 2000.
[6] R.W. Cahn, P. Haasen, E.J. Kramer, B.R.T. Frost (Eds.), Materials Science and Technology – A Comprehensive Treatment, vols. 10A & 10B, VCH Publishers Inc, New York, 1994.
[7] B.R.T. Frost, P.G. Mardon, L.E. Russell, in: Proceedings of the American Nuclear Society Meeting on Plutonium as a Power Reactor Fuel, Richland, WA, 1962, pp. 4.1.
[8] J.P. Mustelier, in: Symposium on the Effects of Irradiation on Solids and Materials for Reactors, Venice, Italy, 1962, pp. 163.
[9] L.C. Walters, B.R. Seidel, J.H. Kittel, Nucl. Technol. 65 (1984) 179.
[10] J.H. Kittel, B.R.T. Frost, J.P. Mustellier, K.Q. Bagley, G.C. Crittenden, J. van Dievoet, J. Nucl. Mater. 204 (1993) 1.
[11] L.C. Walters, J.H. Kittel, Nucl. Technol. 48 (1980) 273.
[12] D.C. Crawford, D.L. Porter, S.L. Hayes, Trans. Am. Nucl. Soc. 94 (2006) 791.
[13] C.E. Stevenson, The EBR-II Fuel Cycle Story, American Nuclear Society, LaGrange Park, IL, 1987.
[14] R.R. Smith, R.G. Matlock, F.D. McGinnis, M. Novick, F.W. Thalgott, A Mechanism Explaining the Instability of EBR-I, Mark III, ANL-6354, Argonne National Laboratory, 1961.

[15] R.R. Smith, J.F. Boland, F.D. McGinnis, M. Novick, F.W. Thalgott, Instability Studies with EBR-I, Mark III, ANL-6266, Argonne National Laboratory, 1960.
[16] R.O. Haroldsen, F.D. McGinnis, M. Novick, R.R. Smith, F.W. Thalgott, Safety Analysis Report, EBR-I, Mark IV, ANL-6411, Argonne National Laboratory, 1963.
[17] S.T. Zegler, M.V. Nevitt, Structures and Properties of Uranium–Fissium Alloys, ANL-6116, Argonne National Laboratory, 1961.
[18] C.E. Lahm, J.F. Koenig, R.G. Pahl, D.L. Porter, D.C. Crawford, J. Nucl. Mater. 204 (1993) 119.
[19] R.D. Leggett, L.C. Walters, J. Nucl. Mater. 204 (1993) 23.
[20] G.L. Hofman, L.C. Walters, T.H. Bauer, Progr. Nucl. Energy 31 (1/2) (1997) 83.
[21] A.L. Pitner, R.B. Baker, J. Nucl. Mater. 204 (1993) 124.
[22] C.M. Walter, G.H. Golden, N.J. Olson, U–Pu–Zr Metal Alloy: A Potential Fuel for LMFBRs, ANL-76-28, Argonne National Laboratory, 1975.
[23] R.G. Pahl, D.L. Porter, C.E. Lahm, G.L. Hofman, Metall. Mater. Trans. A 21A (1990) 1863.
[24] G.L. Hofman, L.C. Walters, Nuclear Materials, Part I, vol. 10A, VCH Publishers Inc, New York, 1994, p. 1.
[25] N.J. Olson, C.M. Walter, W.N. Beck, Nucl. Technol. 28 (1980) 134.
[26] K.J. Miles, in: Proceedings of the International Topical Meeting in Safety of Next Generation Fast Reactors, American Nuclear Society, Seattle, WA, 1988, p. 119.
[27] S.H. Paine, J.H. Kittel, Preliminary Analysis of Fission-induced Dimensional Changes in Single Crystals of Uranium, ANL-5676, Argonne National Laboratory, 1958.
[28] S.N. Buckley, Irradiation Growth in Uranium, AERE-R 5262, Atomic Energy Research Establishment, Harwell, Berkshire, UK, 1966.
[29] E.F. Sturcken, W.R. McDonell, J. Nucl. Mater. 7 (1) (1962) 85.
[30] C.M. Walter, A.K. Chakraborty, J.P. Bacca, P.G. Shewmon, J. Nucl. Mater. 39 (1) (1971) 122.
[31] M.V. Nevitt, S.T. Zegler, J. Nucl. Mater. 1 (1959) 6.
[32] B.R. Seidel, R.E. Einziger, J.F. Koenig, J.I. Sackett, E.M. Dean, G.D. Hudman, L.C. Walters, Request for a Change in Operating Limit 16: Increase in the Burnup Limit of Mark II Elements from 4.7 to 6.0 at.% Burnup Maximum, ANL Report, 1976, pp. 6.6.
[33] J.P. Bacca, M.J. Feldman, G.C. McClellan, C.M. Walter, S.T. Zegler, Trans. Am. Nucl. Soc. 12 (2) (1969) 555.
[34] M. Haas, J.D. Cerchione, R.J. Dunworth, R.M. Fryer, C.W. Wilkes, M.H. Derbidge, Fabrication of Driver-Fuel Elements for EBR-II, ANL-79-38, Argonne National Laboratory, 1979.
[35] B.R. Seidel, R.E. Einziger, In-Reactor Cladding Breach of EBR-II Driver Fuel Elements, Radiation Effects in Breeder Reactor Structural Materials, AIME, Chicago, IL, 1977.
[36] R.G. Pahl, D.L. Porter, D.C. Crawford, L.C. Walters, J. Nucl. Mater. 188 (1992) 3.
[37] G.L. Hofman, R.G. Pahl, C.E. Lahm, D.L. Porter, Metall. Trans. A 21A (1990) 517.
[38] D. Mohr, L.K. Chang, E.E. Feldman, P.R. Betten, H.P. Planchon, Nucl. Eng. Des. 101 (1987) 45.
[39] L. Burris, R.K. Steunenberg, W.E. Miller, in: AICHE Symposium Series No. 254 83, 1987, pp. 135.
[40] Y.I. Chang, Nucl. Technol. 88 (1989) 129.
[41] H.F. Jelinek, N.J. Carson, A.B. Shuck, Manufacture of EBR-II Core I Fuel, ANL-6274, Argonne National Laboratory, 1961.
[42] R.D. Pierce, T.R. Johnson, C.C. McPheeters, J.J. Laidler, J. Met. 45 (1993) 40.
[43] J.J. Laidler, J.E. Battles, W.E. Miller, J.P. Ackerman, E.L. Carls, Progr. Nucl. Energy 31 (1/2) (1997) 131.
[44] H.F. Jelinek, G.M. Iverson, Nucl. Sci. Eng. 12 (1962) 405.
[45] C.W. Wilkes, G.L. Batte, D.B. Tracy, V. Griffiths, EBR-II Fuel Slug Casting Experience, ANL-IFR-73, Argonne National Laboratory, 1987.
[46] D.B. Tracy, S.P. Henslee, N.E. Dodds, K.J. Longua, Trans. Am. Nucl. Soc. 60 (1989) 314.
[47] B.R. Seidel, D.B. Tracy, V. Griffiths, Apparatus for Injection Casting Metallic Nuclear Energy Fuel Rods, US Patent No. 5044811, 1991.
[48] D.C. Crawford, C.E. Lahm, H. Tsai, R.G. Pahl, J. Nucl. Mater. 204 (1993) 157.
[49] L. Leibowitz, E. Veleckis, R.A. Blomquist, A.D. Pelton, J. Nucl. Mater. 154 (1988) 145.
[50] J.J. Frawley, W.F. Moore, A.J. Kiesler, AFS Int. Cast Met. J. 5 (1980) 31.
[51] Analysis of Casting Defects, American Foundrymen's Society, Des Plains, IL, 1966.
[52] R.E. Einziger, B.R. Seidel, Nucl. Technol. 50 (1980) 25.
[53] G.L. Hofman, Nucl. Technol. 47 (1980) 7.
[54] G.L. Hofman, L.C. Walters, T.H. Bauer, Progr. Nucl. Energy 31 (1/2) (1997) 83.
[55] F.A. Garner, S.I. Porollo, A.N. Vorobjev, Yu.V. Konobeev, A.M. Dvoriashim, V.M. Krigan, N.I. Budylkin, E.G. Mironova, in: 19th International Symposium, ASTM STP 1366, 2000, pp. 874.
[56] A. Fissolo, R. Cauvin, J.P. Hugot, V. Levy, in: 14th International Symposium, ASTM STP 1046, 1990, pp. 700.
[57] R.E. Stoller, A.S. Kumar, D.S. Gelles (Eds.), Fracture Toughness and Tensile Properties of Alloy HT9 in Thin Sections Under High Neutron Fluences, ASTM, Philadelphia, PA.
[58] R.G. Pahl, D.L. Porter, C.E. Lahm, G.L. Hofman, Metall. Trans. A 21A (1990) 1863.
[59] C.H. Bachman, H.G. Hottenrott, Rev. Sci. Instrum. 30 (1959) 126.
[60] A.P. Grunwald, Nucl. Sci. Eng. 12 (1962) 419.
[61] G.D. Hudman, L.C. Walters, Analysis of the Leak-detection System for Top Welds of EBR-II Fuel Elements, ANL/EBR-077, Argonne National Laboratory, 1973.
[62] N.E. Dodds, S.P. Hensless, Sodium Bond Defect Investigations, ANL-IFR-131, Argonne National Laboratory, 1990.
[63] E.S. Sowa, E.L. Kimont, Development of a Process for Sodium Bonding of EBR-II Fuel and Blanket Elements, ANL-6384, Argonne National Laboratory, 1961.
[64] D.F. Washburn, J.W. Weber, in: Proceedings of Conference on Reliable Fuels for Liquid Metal Reactors, September 7–11, Tucson, AZ, 1986, pp. 2-1.
[65] R.B. Baker, F.E. Bard, J.L. Ethridge, in: Proceedings of LMR: A Decade of LMR Progress and Promise, November 11–15, Washington D.C., 1990, pp. 184.
[66] J.L. Ethridge, R.B. Baker, R.D. Leggett, A.L. Pitner, A.E. Waltar, in: Proceedings of LMR: A Decade of LMR Progress and Promise, November 11–15, Washington D.C., 1990, pp. 163.
[67] D.E. Burkes, R.S. Fielding, D.L. Porter, M.K. Meyer, B.J. Makenas, J. Nucl. Mater., submitted for publication.